

Article

Catalytic Steam Reforming of Toluene as a Model Compound of Biomass Gasification Tar Using Ni-CeO₂/SBA-15 Catalysts

Jun Tao ¹, Leiqiang Zhao ¹, Changqing Dong ¹, Qiang Lu ^{1,*}, Xiaoze Du ² and Erik Dahlquist ³

¹ National Engineering Laboratory for Biomass Power Generation Equipment, North China Electric Power University, No.2 Beinong Road, Changping District, Beijing 102206, China; E-Mails: firsttaojun@163.com (J.T.); zhaoleiqiang@126.com (L.Z.); cqdong1@163.com (C.D.)

² Key Laboratory of Condition Monitoring and Control for Power Plant Equipment, Ministry of Education, North China Electric Power University, No.2 Beinong Road, Changping District, Beijing 102206, China; E-Mail: duxz@ncepu.edu.cn

³ School of Sustainable Development of Society and Technology, Mälardalen Univeristy, Västerås, SE-721 23, Sweden; E-Mail: erik.dahlquist@mdh.se

* Author to whom correspondence should be addressed; E-Mail: qianglu@mail.ustc.edu.cn; Tel.: +86-10-6177-2063; Fax: +86-10-6177-2032 (ext. 801).

Received: 6 May 2013; in revised form: 16 June 2013 / Accepted: 27 June 2013 /

Published: 4 July 2013

Abstract: Nickel supported on SBA-15 doped with CeO₂ catalysts (Ni-CeO₂/SBA-15) was prepared, and used for steam reforming of toluene which was selected as a model compound of biomass gasification tar. A fixed-bed lab-scale set was designed and employed to evaluate the catalytic performances of the Ni-CeO₂/SBA-15 catalysts. Experiments were performed to reveal the effects of several factors on the toluene conversion and product gas composition, including the reaction temperature, steam/carbon (S/C) ratio, and CeO₂ loading content. Moreover, the catalysts were subjected to analysis of their carbon contents after the steam reforming experiments, as well as to test the catalytic stability over a long experimental period. The results indicated that the Ni-CeO₂/SBA-15 catalysts exhibited promising capabilities on the toluene conversion, anti-coke deposition and catalytic stability. The toluene conversion reached as high as 98.9% at steam reforming temperature of 850 °C and S/C ratio of 3 using the Ni-CeO₂(3wt%)/SBA-15 catalyst. Negligible coke formation was detected on the used catalyst. The gaseous products mainly consisted of H₂ and CO, together with a little CO₂ and CH₄.

Keywords: steam reforming; biomass gasification tar; toluene; Ni-CeO₂/SBA-15

1. Introduction

The utilization of lignocellulosic biomass has gained attention in recent years [1–3]. Among the various conversion technologies, gasification is a promising one to convert solid biomass mainly into a gaseous product rich in H₂ and CO which can be used as a gaseous fuel or a raw material for Fischer-Tropsch synthesis [4–6]. A major problem involved in the gasification process is the formation of tar which is a complex mixture of various organic compounds, especially aromatic compounds. Tars would bring many negative effects to the operation of the gasification equipment as well as the downstream gas utilization engines or turbines. Therefore, it is very essential to remove tars for the commercialization of the biomass gasification technique.

There are several methods to remove tars. One of them is catalytic steam reforming which can convert tar compounds in the presence of steam to permanent gases, with high energy recovery and minimal environmental pollution [7,8]. The key problem for catalytic steam reforming is the selection of the proper catalyst. Till now, various catalysts have been prepared and tested, mainly including the olivine and dolomite [9–11], Ni-based catalysts [12–14] and noble metal catalysts [15]. Among these catalysts, Ni-based catalysts were confirmed to be effective for tar reduction, due to the promising cracking capability of the NiO/Ni [8,16–18]. For instance, Zhao *et al.* [19] prepared Ni/cordierite catalysts for steam reforming of toluene which was selected as a model tar compound. The results indicated that the toluene conversion would be enhanced with the increase of reforming temperature, reaching as high as 94.1% at 900 °C. Zhang *et al.* [20] prepared Ni/olivine catalysts doped with CeO₂ for steam reforming of model tar compounds (benzene and toluene), and found that the catalysts were effective in terms of both catalytic activity and anti-coke deposition performances.

However, during the catalytic process, the Ni-based catalysts would deactivate very rapidly, mainly resulting from the coke deposition. Hence, it is essential to improve the anti-coke deposition performances of the Ni-based catalysts. In this study, nickel supported on SBA-15 doped with CeO₂ (Ni-CeO₂/SBA-15) catalysts were prepared for steam reforming of biomass gasification tars. The CeO₂ was selected as the catalyst promoter, because it is preliminarily confirmed to be effective to prevent coke deposition and stabilize the catalysts, due to the strong metal support interaction of the Ni-CeO₂ system [20]. The CeO₂ can accelerate the reaction of steam and absorbed species on nickel surface near the boundary area, so that carbon deposited on the surface can be quickly converted to gaseous products, preventing its accumulation. Moreover, SBA-15 was selected as the catalyst support, because it is a highly ordered mesoporous material which has much larger pore size (3–30 nm) than those of traditional microporous catalysts (<2 nm) [21–23]. The large pore size makes the mesoporous SBA-15 very promising to convert large molecule compounds, since the traditional microporous catalysts are unable to treat the large molecules (including tars). The SBA-15 also has good thermal and hydrothermal stability, further making it a promising support for various catalysts [24,25].

In this study, a lab-scale setup was designed and established for steam reforming experiments using the Ni-CeO₂/SBA-15 catalysts. To better understand the catalytic performances of the

Ni-CeO₂/SBA-15 catalysts, toluene was selected as the model tar compound for experiments, because it is a major and stable tar compound formed in the high temperature gasification process. Experiments were performed to reveal the effects of the reaction temperature, S/C ratio, and CeO₂ loading content on the toluene conversion and product distribution.

2. Experimental

2.1. Catalyst Preparation

The SBA-15 was synthesized by the sol-gel method [21]. Typically, a homogeneous mixture composed of block copolymer surfactant (Pluronic P123; PEO₂₀PPO₇₀PEO₂₀) and tetraethyl orthosilicate (TEOS) in hydrochloric acid was stirred at 40 °C for 24 h and then crystallized in a Teflon-lined autoclave at 100 °C for 2 days. The resultant solid was filtered, washed and dried. After calcination in air at 550 °C for 4 h, the white SBA-15 powders were obtained and used as the catalyst supports for the preparation of the Ni/SBA-15 and Ni-CeO₂/SBA-15 catalysts.

The Ni/SBA-15 and Ni-CeO₂/SBA-15 catalysts were prepared by one step incipient wetness impregnation method [26]. To prepare the Ni-SBA-15 catalyst, 1.5 g nickel nitrate hexahydrate was firstly dissolved in 53 mL deionized water. Afterwards, 9.7 g SBA-15 was added to the above solution with ultrasonic treatment for 12 h. The mixture was then dried at 105 °C in air for 12 h. To prepare the Ni-CeO₂/SBA-15 catalysts, 1.5 g nickel nitrate hexahydrate and certain amount of cerium nitrate hexahydrate (0.3 g or 0.8 g) were dissolved in certain amount of de-ionized water (53 mL or 52 mL), followed with the addition of certain amount of SBA-15 (9.6 g or 9.4 g) with ultrasonic treatment for 12 h. The mixture was then dried at 105 °C in air for 12 h. The above resultant solids after drying were not calcined in air, but directly calcined in the mixture of nitrogen and hydrogen before catalytic activity tests, because calcination in air prior to the reduction step would be detrimental to obtain high reducibility, metal surface area, and metal dispersion of the Ni-based catalysts [27]. The nickel loading for all the catalysts was fixed at 3 wt% and the CeO₂ loading was 0 wt%, 1wt% and 3 wt%, respectively.

2.2. Catalyst Characterization

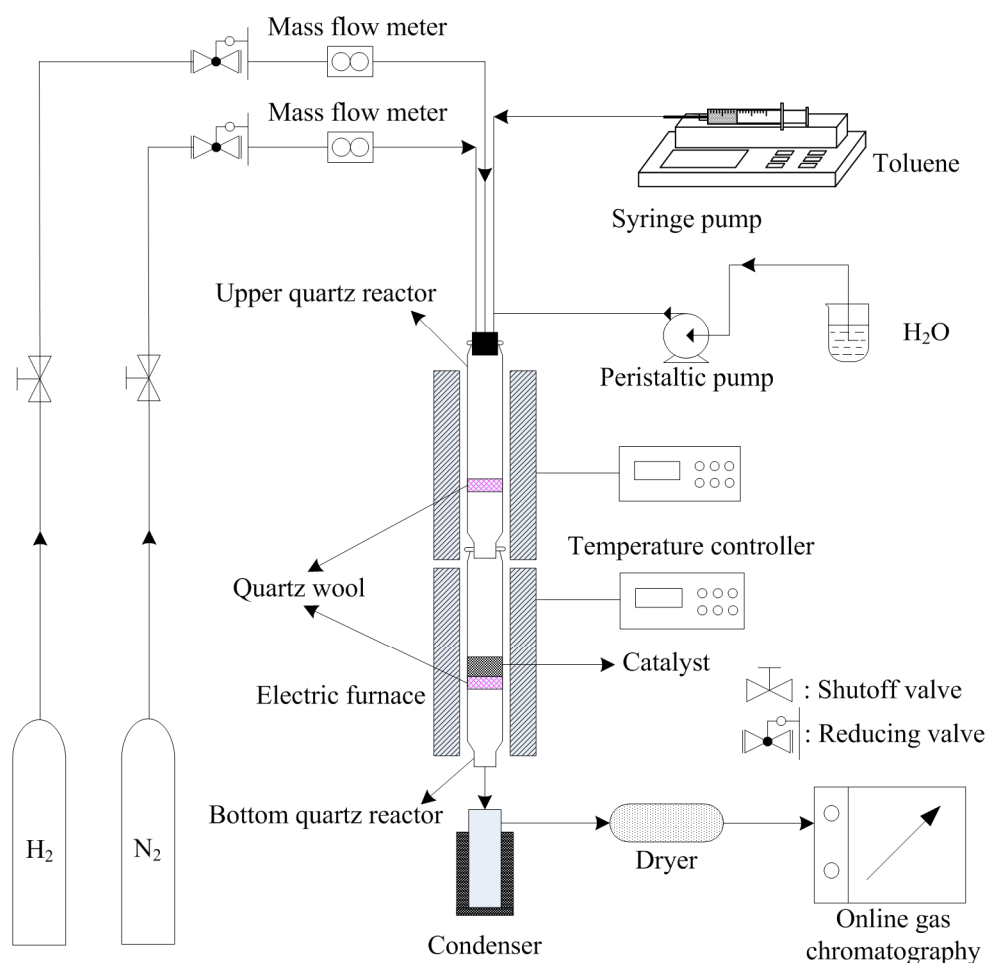
Nitrogen adsorption and desorption isotherms of the catalysts were obtained at 77 K on the Quantachrome Autosorb-iQ physical adsorption instrument. Specific surface area and pore volume were calculated using Brunauer–Emmett–Teller (BET) equation and Barrett–Joyner–Halenda (BJH) method, respectively. The crystalline structures of the catalysts were assessed on a Rigaku Rotaflex diffractometer, using the Cu K α radiation ($\lambda = 0.15406$ nm). Small-angle and wide-angle XRD patterns were measured over the 2θ range of 0.9~6° and 10~80°. Moreover, after catalytic steam reforming experiments, the carbon contents of the catalysts were determined by a Vario Macro Cube Elemental Analyzer.

2.3. Catalytic Steam Reforming Experiments

A lab-scale experimental setup was designed and used for steam reforming of toluene, as shown in Figure 1. The setup mainly consisted of a syringe pump, a peristaltic pump, an upper quartz reactor, a bottom quartz reactor, an ice-cooled condenser, and an on-line gas analyzer (INFICON 3000 Micro

gas chromatograph; INFICON, East Syracuse, NY, USA). The syringe pump and peristaltic pump were used to inject the liquid toluene and water which were then heated and evaporated in the upper quartz reactor (i.d. 15 mm). The bottom reactor (i.d. 15 mm) was used for steam reforming of the toluene, and 0.5 g uncalcined catalyst was filled in it and placed above some quartz wool at the uniform temperature zone. The upper and bottom quartz reactors were vertically positioned in two separate heating furnaces which were used to heat the two reactors. The temperatures of the two reactors were monitored by thermocouples.

Figure 1. Schematic of the toluene steam reforming set.



During the experiments, before the injection of the toluene and water, the catalyst was firstly calcined in the mixture of 50 vol% H₂ and 50 vol% N₂ with the flow rate of 120 mL/min. The calcination was programmed from room temperature to 850 °C at the heating rate of 2 °C/min, and then held at 850 °C for 6 h, to obtain the Ni/SBA-15 or Ni-CeO₂/SBA-15 catalyst. After the calcination, only N₂ was used as the carrier gas for the steam reforming experiments. Toluene and water were injected to the upper quartz reactor which was heated to 300 °C. The feeding rates of the N₂ (g), H₂O (g) and toluene (g), corresponding to the gaseous state at 25 °C, were 29.7–40.8 mL/min, 7.4–18.5 mL/min and 0.53 mL/min, respectively. The concentration of the toluene in the gas flow was fixed at 45 g/Nm³ (1.1 vol.%), in order to perform catalytic steam reforming experiments under severe conditions [28]. The S/C ratio was in the range of 2–5. The space time ($w_{\text{cat}}/F_{\text{toluene}}$) at 25 °C, defined

in terms of the catalyst weight divided to the volumetric flow rate of the toluene vapor, was $16 \text{ kg}_{\text{cat}}\text{h}/\text{m}^3$ [29]. The nitrogen flow was controlled by a mass flowmeter and adjusted according to the H_2O (g) content in the feeding mixture to keep the constant space time. The catalytic temperature was ranged from $700 \text{ }^\circ\text{C}$ to $850 \text{ }^\circ\text{C}$, similar as the practical gasifier. The effluent gases from the reactor were condensed in the ice-cooled condenser to collect the un-reacted toluene and water. The non-condensable gases were then dried by the CaCl_2 column, and analyzed by the INFICON 3000 Micro gas chromatograph which was equipped with four detection modules, to measure the H_2 , CO , CO_2 , N_2 and $\text{C}_1\text{--C}_3$ hydrocarbons. Each gas analysis was completed in 2.8 min. Each steam reforming experiment lasted for 4 h, resulting in around 85 measurements for each test. After the 4 h experiment, the injection of toluene and water was firstly stopped while nitrogen was still fed to cool down the catalyst to room temperature, preventing the catalyst being oxidized by the oxygen in air. Finally, the used catalyst was collected and subjected to further characterization.

2.4. Data Analysis

The H_2 , CO , CO_2 , CH_4 and N_2 were detected in each gas analysis, and their contents were determined, while the $\text{C}_2\text{--C}_3$ hydrocarbons were not detected. For each steam reforming test, the average values of the H_2 , CO , CO_2 and CH_4 contents from the 85 measurements were calculated. It is note that the nitrogen flow rate was fixed during each steam reforming test, and thus, based on the calculated average N_2 content, it is able to calculate the yields of the H_2 , CO , CO_2 and CH_4 in each experiment.

Based on the gaseous products, the toluene conversion ($X_{\text{C}_7\text{H}_8}$) could be calculated according to Equation (1), which was defined in terms of the carbon in the gas products (CO , CO_2 , CH_4) divided to the carbon in the toluene. The hydrogen content ($\text{V}\%(\text{H}_2)$) was calculated according to Equation (2), and the contents of the other gases were calculated in the same way:

$$X_{\text{C}_7\text{H}_8} (\text{mol}\%) = \frac{F_{\text{CO,out}} + F_{\text{CO}_2,\text{out}} + F_{\text{CH}_4,\text{out}}}{7F_{\text{C}_7\text{H}_8,\text{in}}} \times 100 \quad (1)$$

$$\text{V}\%(\text{H}_2) = \frac{\text{H}_2}{\text{H}_2 + \text{CO} + \text{CO}_2 + \text{CH}_4} \times 100 \quad (2)$$

3. Results and Discussion

3.1. Catalyst Characterization

The N_2 adsorption/desorption isotherms of the SBA-15, Ni/SBA-15 and Ni- CeO_2 /SBA-15 catalysts are shown in Figure 2. The SBA-15 exhibited a typical irreversible type IV adsorption isotherm with a standard H1 hysteresis loop, and a sharp inflection at the relative pressure (p/p_0) of 0.58, implying this material had regular mesoporous channels. The Ni/SBA-15 and Ni- CeO_2 /SBA-15 catalysts showed similar isotherms as the SBA-15, indicating that they retained the regular mesoporous structure of the parent SBA-15.

The textural properties of the catalysts are listed in Table 1. The Ni/SBA-15 and Ni- CeO_2 /SBA-15 catalysts had lower surface areas, smaller pore volumes and average pore diameters than the SBA-15, which should be due to the occupation of the Ni and CeO_2 particles in the pore channels. Nevertheless,

the two Ni-CeO₂/SBA-15 catalysts possessed better textural properties than the Ni/SBA-15 catalyst, which might be due to the better nickel dispersion and smaller nickel particle sizes in the presence of the CeO₂, as has been previously reported [30].

Figure 2. N₂ adsorption/desorption isotherms with BJH pore size distribution analysis. (a) SBA-15; (b) Ni/SBA-15; (c) Ni-CeO₂ (1 wt%)/SBA-15; and (d) Ni-CeO₂ (3 wt%)/SBA-15.

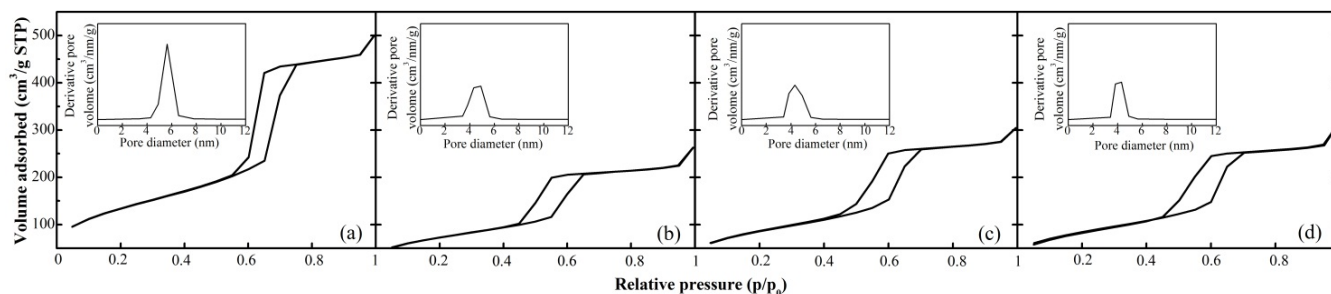


Table 1. Textural properties of the catalysts.

Sample	BET Surface area (m ² /g)	Pore volume (cm ³ /g)	Average pore diameter (nm)
SBA-15	476.4	0.76	5.63
Ni/SBA-15	261.1	0.43	4.31
Ni-CeO ₂ (1wt%)/SBA-15	301.6	0.48	4.32
Ni-CeO ₂ (3wt%)/SBA-15	307.7	0.51	4.89

Figure 3 gives the small-angle XRD patterns of the catalysts. The SBA-15 displayed an intense peak and two weak peaks for the mesoporous silica (100), (110) and (200) planes, respectively. This pattern indicated a 2D hexagonal mesostructure with space group p6 mm, matched well with the pattern reported for SBA-15 [21]. Similar diffraction peaks were observed for the Ni/SBA-15 and Ni-CeO₂/SBA-15 catalysts, but these peaks were shifted to higher 2θ values, which might be due to the incorporation of the Ni and CeO₂ on the SBA-15 [31]. Moreover, the intensities of the diffraction peaks were decreased, which might be attributed to the partial degradation of the hexagonal arrangement of SBA-15 pores [32] or the dilution of the silica by the nickel which has a higher absorption factor of X-rays than the silicon [33].

Figure 4 gives the wide-angle XRD patterns of the catalysts. The broad diffraction peak at about 2θ = 23° was attributed to the amorphous SiO₂ [22]. The diffraction peaks at 2θ of 44.5° and 51.8° were assigned as the characteristic peaks of metallic nickel, JCPDS database (No. 01-1258) [30]. It is seen that in the presence of the CeO₂, these peaks were broadened and their intensities were decreased, indicating the improved dispersion of the metallic phase. The crystalline size of the Ni⁰ phase, calculated according to the Scherrer equation from the characteristic peak at 44.5°, was reduced from 8.4 nm for the Ni/SBA-15 catalyst to 4.9 nm for the Ni-CeO₂(3wt%)/SBA-15 catalyst. The above results confirmed that the CeO₂ could promote the dispersion of the Ni particles, agreed with previous studies [25,30]. This fact should be at least partly responsible for the better textural properties of the Ni-CeO₂/SBA-15 catalysts than the Ni/SBA-15 catalyst.

Figure 3. Small-angle XRD patterns of the catalysts. (a) SBA-15; (b) Ni/SBA-15; (c) Ni-CeO₂(1wt%)/SBA-15; and (d) Ni-CeO₂(3wt%)/SBA-15.

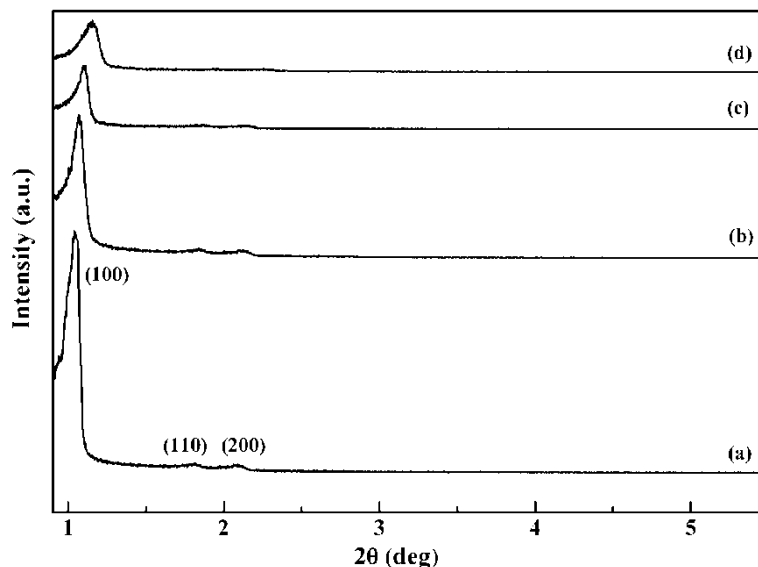
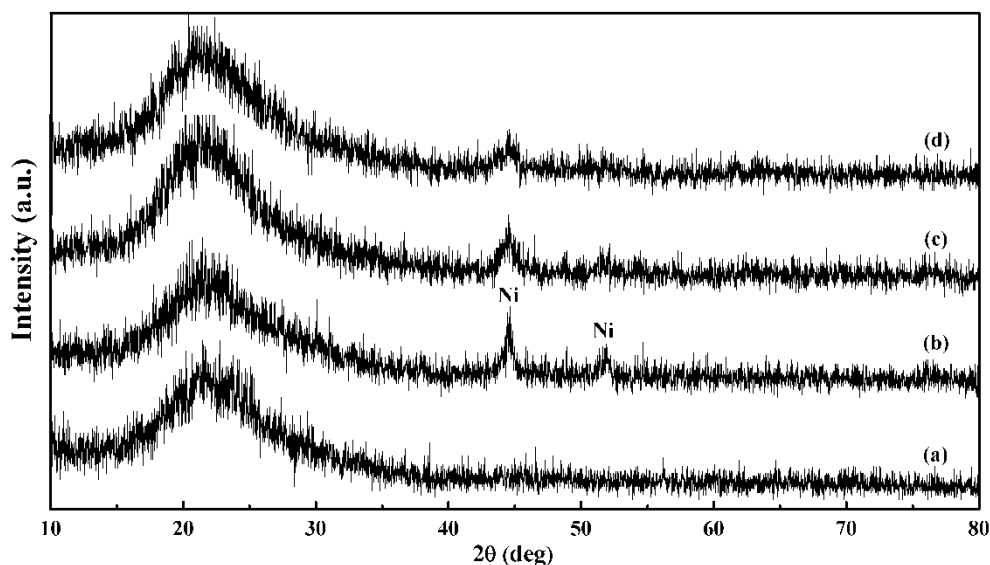


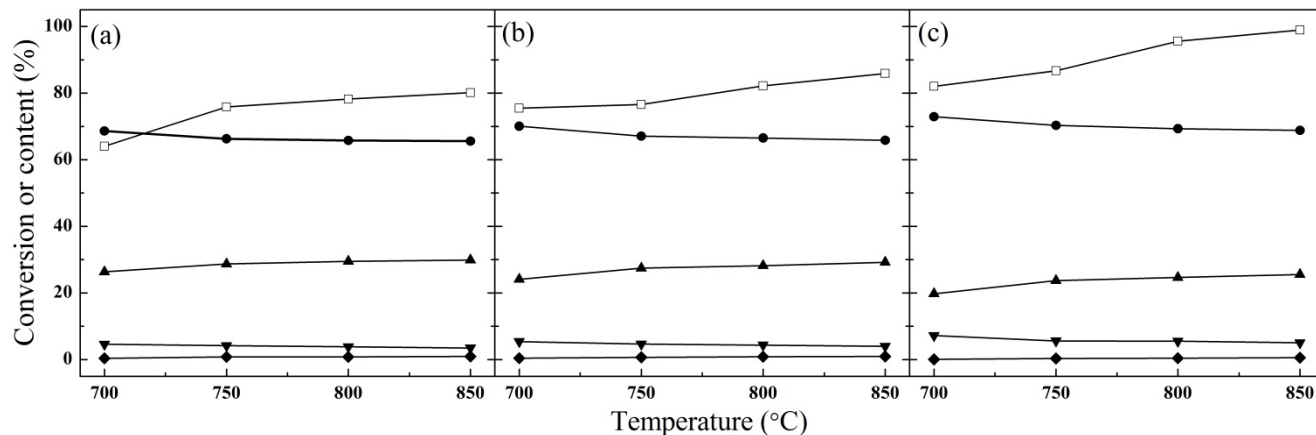
Figure 4. Wide-angle XRD patterns of the catalysts. (a) SBA-15; (b) Ni/SBA-15; (c) Ni-CeO₂(1 wt%)/SBA-15; and (d) Ni-CeO₂(3 wt%)/SBA-15.



3.2. Effects of Catalytic Temperature and CeO₂ Loading Content on the Steam Reforming of Toluene

Figure 5 illustrates the effects of catalytic temperatures on the steam reforming of toluene over different catalysts in the temperature range of 700–850 °C with the S/C ratio of 3. No catalyst deactivation was observed during the 4 h test for either catalyst. According to Figure 5, the toluene conversion was enhanced with an increase in the temperature and the CeO₂ loading content. The highest toluene conversion reached as high as 98.9% at 850 °C using the Ni-CeO₂(3 wt%)/SBA-15 catalyst. The results clearly indicated the Ni-CeO₂/SBA-15 catalyst had promising catalytic capability to convert the toluene, and the CeO₂ loading was capable to promote the catalytic activity.

Figure 5. Effects of reaction temperatures on the toluene conversion and the gas composition. (a) Ni/SBA-15; (b) Ni-CeO₂(1 wt%)/SBA-15; and (c) Ni-CeO₂(3 wt%)/SBA-15. (□) toluene conversion; (●) H₂ content; (▲) CO content; (▼) CO₂ content; and (◆) CH₄ content.



The steam reforming of toluene generated the H₂ and CO as the major products, together with CO₂ and CH₄ as the minor products. According to Figure 5, the contents of these gas products were remarkably affected by the catalytic temperature, but not greatly influenced by the CeO₂ loading content. The CO content was increased monotonically along with the catalytic temperature, from 19.8% at 700 °C to 25.5% at 850 °C using the Ni-CeO₂ (3 wt%)/SBA-15 catalyst. The H₂ and CO₂ contents were changed oppositely, decreased from 72.9% and 7.3% at 700 °C to 68.8% and 5.0% at 850 °C, respectively. This might be attributed to the temperature improved reverse water gas shift reaction ($\text{CO} + \text{H}_2\text{O} \leftrightarrow \text{H}_2 + \text{CO}_2$). Due to the exothermal nature of the water gas shift reaction, the increase of temperature would favor the formation of CO on the expense of H₂ and CO₂ [19]. The CH₄ content was below 1.0%, and almost kept constant under different catalytic temperatures.

The catalysts after 4 h catalytic steam reforming tests were analyzed to measure their carbon contents, and the results are shown in Table 2. It is seen that the carbon content was gradually decreased along with the catalytic temperature and the CeO₂ loading content. The least carbon content was observed for the Ni-CeO₂ (3 wt%)/SBA-15 catalyst under the catalytic temperature of 850 °C, with the value of only 0.01 wt%, which was negligible. The above results clearly indicated that the presence of the CeO₂ could improve the anti-coke deposition performances of the catalysts.

Table 2. Carbon contents of the three used catalysts under different reaction temperatures.

Sample	Carbon content under different temperatures (wt%)			
	700 °C	750 °C	800 °C	850 °C
Ni/SBA-15	0.31	0.28	0.25	0.21
Ni-CeO ₂ (1wt%)/SBA-15	0.12	0.11	0.05	0.02
Ni-CeO ₂ (3wt%)/SBA-15	0.09	0.08	0.05	0.01

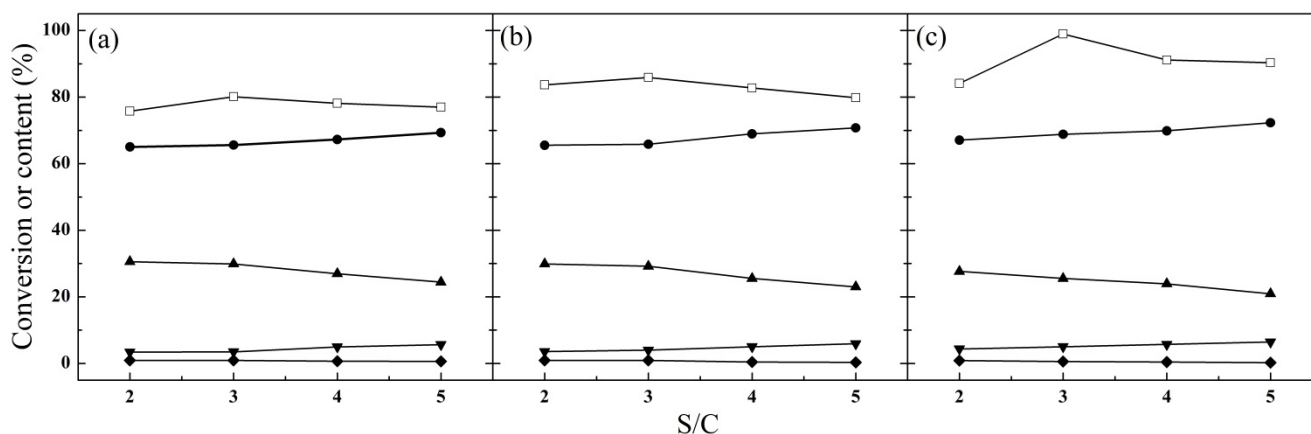
It was previously reported that an active catalyst for steam reforming of tar compounds should be effective to cleavage the C-C bond and also promote the water gas shift reaction [34]. Although the metal Ni was able to catalyze the C-C bond cleavage, it was not very capable to promote the water gas

shift reaction and to resist coke deposition. The CeO₂ was known for its oxygen storage and release ability [35], and thus, could be used as the catalytic promoter to enhance the anti-coke deposition performances of the catalysts. Therefore, the Ni-CeO₂/SBA-15 catalysts had more promising effects than the Ni/SBA-15 catalyst to convert toluene and to resist coke deposition.

3.3. Effects of the S/C Ratio on the Steam Reforming of Toluene

Figure 6 shows the effects of S/C ratios on the steam reforming of toluene using the three catalysts at 850 °C. The S/C ratio had profound effects on the toluene conversion and the gas composition. According to Figure 6, with the increase of the S/C ratio from 2 to 5, the toluene conversion was firstly increased and then decreased, and the maximal toluene conversion was obtained at the S/C ratio of 3. In regard to the gas products, the H₂ and CO₂ contents were steadily increased along with the S/C ratio, while the CO and CH₄ contents were monotonically decreased. This phenomenon might be explained by the toluene steam reforming reaction ($C_7H_8 + 14H_2O \rightarrow 7CO_2 + 18H_2$) and water gas shift reaction. During the steam reforming process, the toluene and water molecules were absorbed on the catalyst surface, reacting to form CO or CO₂. At the high S/C ratio, most of the active sites of the catalyst surface would be occupied by the H₂O molecules [34], resulting in the decreased adsorption and conversion of the toluene. Nevertheless, the high water concentration would promote the water gas shift reaction towards the formation of the H₂ and CO₂. Based on Figure 6, the S/C ratio of 3 was the optimal condition for the toluene conversion and product gas composition.

Figure 6. Effects of S/C ratios on the toluene conversion and the gas composition. (a) Ni/SBA-15; (b) Ni-CeO₂ (1 wt%)/SBA-15; and (c) Ni-CeO₂ (3 wt%)/SBA-15. (□) toluene conversion; (●) H₂ content; (▲) CO content; (▼) CO₂ content; and (◆) CH₄ content.



Various catalysts have been prepared for steam reforming of toluene in previous studies. The catalytic performances of those previously reported catalysts (No.1-7) and our Ni-CeO₂ (3 wt%)/SBA-15 catalyst (No.8) are given in Table 3. It is clear that the Ni-CeO₂/SBA-15 is an effective catalyst with promising toluene conversion capability.

Table 3. Comparison of the catalytic performances of previously reported catalysts and the Ni-CeO₂(3wt%)/SBA-15 catalyst.

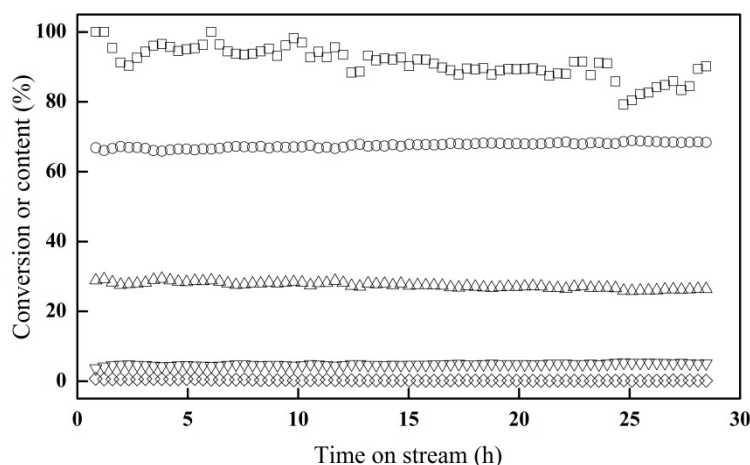
No.	Catalyst	Temperature (°C)	S/C	Space time	Toluene conversion (%)	Ref.
1	Fe/MgO	850	18:7	20 kg _{cat} h/m ³ [a]	77	[36]
2	NiO-CeO ₂ /Olivine	830	5:1	862 h ⁻¹ [b]	77.9	[20]
3	Fe/Olivine	850	15:7	16.7 kg _{cat} h/m ³ [a]	85	[29]
4	Ni/cordierite	900	2:1	-	94.1	[19]
5	Ni/Al/La	650	5.7:1	1326 h ⁻¹ [c]	94.53	[37]
6	Cordierite	900	1.5:1	1031 h ⁻¹ [b]	95	[38]
7	Ni/Olivine	650	2.3:1	9 kg _{cat} h/m ³ [a]	100	[39]
8	Ni-CeO ₂ /SBA-15	850	3:1	16 kg _{cat} h/m ³ [a]	98.9	-

[a] Defined in terms of the catalyst weight divided to the volumetric flow rate of toluene vapor; [b] Defined in terms of the catalyst bed volume divided to the volumetric flow rate of the total vapor; [c] Defined in terms of the catalyst weight divided to the mass flow rate of toluene.

3.4. Catalytic Stability Test

Experiments were also conducted to evaluate the catalytic stability of the Ni-CeO₂ (3 wt%)/SBA-15 catalyst at the S/C ratio of 3 and catalytic temperature of 850 °C, which were the best catalyst and reaction condition for toluene conversion. The catalytic stability test lasted for 29 h, and the results are shown in Figure 7. It is seen that the Ni-CeO₂(3wt%)/SBA-15 catalyst almost maintained its excellent catalytic activity, and the toluene conversion was only slightly reduced during the whole test. This might be due to the small amount of coke deposition on the quartz reactor (not on the catalyst), which was observed after the stability test. Meanwhile, the contents of H₂ and CO₂ were increased very slightly, while the contents of CO and CH₄ dropped only a little. The carbon content of the used catalyst was only 0.01 wt%, which was negligible. The above results clearly indicated that the Ni-CeO₂(3wt%)/SBA-15 catalyst possessed promising anti-coke deposition performance and catalytic stability.

Figure 7. Catalytic stability test for steam reforming of toluene using Ni-CeO₂ (3 wt%)/SBA-15 catalyst. (□) toluene conversion; (○) H₂ content; (Δ) CO content; (∇) CO₂ content; and (◇)CH₄ content.



4. Conclusions

In this study, Ni-CeO₂/SBA-15 catalysts were prepared for steam reforming of toluene, and they exhibited promising capabilities on the toluene conversion, anti-coke deposition as well as catalytic stability. During the catalytic steam reforming process, the toluene conversion was steadily enhanced with the increase of the catalytic temperature and the CeO₂ loading content. Moreover, the toluene conversion was firstly increased and then decreased along with the S/C ratio, with the maximal value obtained at the S/C ratio of 3. The Ni-CeO₂ (3 wt%)/SBA-15 catalyst possessed the best catalytic activity, with the maximal toluene conversion as high as 98.9% at the catalytic temperature of 850 °C and S/C ratio of 3. Moreover, this catalyst also showed promising catalytic stability during the long period stability test, and negligible coke formation was detected on the used catalyst. The gas products from the steam reforming process were mainly H₂ and CO, together with a little of CO₂ and CH₄. The H₂ content in the gas products would be gradually decreased with the increase of the catalytic temperature, while the CO content would be gradually increased.

Acknowledgments

The authors thank the National Natural Science Foundation of China (51276062, 51106052), National Key Technology R&D Program (2012BAD30B01), Program for New Century Excellent Talents in University (NCET-10-0374), 111 Project (B12034), and Fundamental Research Funds for the Central Universities (11ZG08, 12ZP02, 13ZP02) for financial support.

Conflict of Interest

The authors declare no conflict of interest.

References

1. Ball, M.; Wietschel, M. The future of hydrogen-opportunities and challenges. *Int. J. Hydrog. Energy* **2009**, *34*, 615–627.
2. Haykiri-Acma, H.; Yaman, S. Thermogravimetric investigation on the thermal reactivity of biomass during slow pyrolysis. *Int. J. Green Energy* **2009**, *6*, 333–342.
3. Gezer, I.; Dođru, M.; Akay, G. Gasification of apricot pit shells in a downdraft gasifier. *Int. J. Green Energy* **2009**, *6*, 218–227.
4. Yin, R.; Liu, R.; Wu, J.; Wu, X.; Sun, C.; Wu, C. Influence of particle size on performance of a pilot-scale fixed-bed gasification system. *Bioresour. Technol.* **2012**, *119*, 15–21.
5. Nguyen, T.D.B.; Ngo, S.I.; Lim, Y.-I.; Lee, J.W.; Lee, U.-D.; Song, B.-H. Three-stage steady-state model for biomass gasification in a dual circulating fluidized-bed. *Energy Convers. Manag.* **2012**, *54*, 100–112.
6. Huang, B.-S.; Chen, H.-Y.; Kuo, J.-H.; Chang, C.-H.; Wey, M.-Y. Catalytic upgrading of syngas from fluidized bed air gasification of sawdust. *Bioresour. Technol.* **2012**, *110*, 670–675.
7. Wang, L.; Hisada, Y.; Koike, M.; Li, D.; Watanabe, H.; Nakagawa, Y.; Tomishige, K. Catalyst property of Co-Fe alloy particles in the steam reforming of biomass tar and toluene. *Appl. Catal. B Environ.* **2012**, *121–122*, 95–104.

8. Yang, X.Q.; Xu, S.P.; Xu, H.L.; Liu, X.D.; Liu, C.H. Nickel supported on modified olivine catalysts for steam reforming of biomass gasification tar. *Catal. Commun.* **2010**, *11*, 383–386.
9. Devi, L.; Ptasinski, K.J.; Janssen, F.J.J.G. Pretreated olivine as tar removal catalyst for biomass gasifiers: Investigation using naphthalene as model biomass tar. *Fuel Process. Technol.* **2005**, *86*, 707–730.
10. Yu, Q.Z.; Brage, C.; Nordgreen, T.; Sjöström, K. Effects of Chinese dolomites on tar cracking in gasification of birch. *Fuel* **2009**, *88*, 1922–1926.
11. Devi, L.; Ptasinski, K.J.; Janssen, F.J.J.G.; van Paasen, S.V.B.; Bergman, P.C.A.; Kiel, J.H.A. Catalytic decomposition of biomass tars: Use of dolomite and untreated olivine. *Renew. Energy* **2005**, *30*, 565–587.
12. Park, H.J.; Park, S.H.; Sohn, J.M.; Park, J.; Jeon, J.-K.; Kim, S.-S.; Park, Y.-K. Steam reforming of biomass gasification tar using benzene as a model compound over various Ni supported metal oxide catalysts. *Bioresour. Technol.* **2010**, *101*, S101–S103.
13. Li, C.S.; Hirabayashi, D.; Suzuki, K. Steam reforming of biomass tar producing H₂-rich gases over Ni/MgO_x/CaO_{1-x} catalyst. *Bioresour. Technol.* **2010**, *101*, S97–S100.
14. Zhao, Z.K.; Kuhn, J.N.; Felix, L.G.; Slimane, R.B.; Choi, C.W.; Ozkan, U.S. Thermally impregnated Ni-olivine catalysts for tar removal by steam reforming in biomass gasifiers. *Ind. Eng. Chem. Res.* **2008**, *47*, 717–723.
15. Colby, J.L.; Wang, T.; Schmidt, L.D. Steam reforming of benzene as a model for biomass-derived syngas tars over rh-based catalysts. *Energy Fuel* **2009**, *24*, 1341–1346.
16. Li, C.; Hirabayashi, D.; Suzuki, K. Development of new nickel based catalyst for biomass tar steam reforming producing H₂-rich syngas. *Fuel Process. Technol.* **2009**, *90*, 790–796.
17. Łamacz, A.; Krztoń, A.; Djéga-Mariadassou, G. Steam reforming of model gasification tars compounds on nickel based ceria-zirconia catalysts. *Catal. Today* **2011**, *176*, 347–351.
18. Yan, C.-F.; Cheng, F.-F.; Hu, R.-R. Hydrogen production from catalytic steam reforming of bio-oil aqueous fraction over Ni/CeO₂-ZrO₂ catalysts. *Int. J. Hydrog. Energy* **2010**, *35*, 11693–11699.
19. Zhao, B.F.; Zhang, X.D.; Chen, L.; Qu, R.B.; Meng, G.F.; Yi, X.L.; Sun, L. Steam reforming of toluene as model compound of biomass pyrolysis tar for hydrogen. *Biomass Bioenergy* **2010**, *34*, 140–144.
20. Zhang, R.Q.; Wang, Y.C.; Brown, R.C. Steam reforming of tar compounds over Ni/olivine catalysts doped with CeO₂. *Energ. Convers. Manag.* **2007**, *48*, 68–77.
21. Zhao, D.; Feng, J.; Huo, Q.; Melosh, N.; Fredrickson, G.H.; Chmelka, B.F.; Stucky, G.D. Triblock copolymer syntheses of mesoporous silica with periodic 50 to 300 angstrom pores. *Science* **1998**, *279*, 548–552.
22. Zhao, D.; Huo, Q.; Feng, J.; Chmelka, B.F.; Stucky, G.D. Nonionic triblock and star diblock copolymer and oligomeric surfactant syntheses of highly ordered, hydrothermally stable, mesoporous silica structures. *J. Am. Chem. Soc.* **1998**, *120*, 6024–6036.
23. Zhao, D.; Sun, J.; Li, Q.; Stucky, G.D. Morphological control of highly ordered mesoporous silica SBA-15. *Chem. Mater.* **2000**, *12*, 275–279.
24. Huang, B.; Li, X.; Ji, S.; Lang, B.; Habimana, F.; Li, C. Effect of MgO promoter on Ni-based SBA-15 catalysts for combined steam and carbon dioxide reforming of methane. *J. Nat. Gas. Chem.* **2008**, *17*, 225–231.

25. Wan, H.; Li, X.; Ji, S.; Huang, B.; Wang, K.; Li, C. Effect of Ni loading and $Ce_xZr_{1-x}O_2$ promoter on Ni-Based SBA-15 catalysts for steam reforming of methane. *J. Nat. Gas. Chem.* **2007**, *16*, 139–147.
26. Li, D.; Nakagawa, Y.; Tomishige, K. Development of Ni-based catalysts for steam reforming of tar derived from biomass pyrolysis. *Chin. J. Catal.* **2012**, *33*, 583–594.
27. Bartholomew, C.H.; Farrauto, R.J. Chemistry of nickel-alumina catalysts. *J. Catal.* **1976**, *45*, 41–53.
28. Brown, M.D.; Baker, E.G.; Mudge, L.K. Environmental design considerations for thermochemical biomass energy. *Biomass* **1986**, *11*, 255–270.
29. Virginie, M.; Courson, C.; Kiennemann, A. Toluene steam reforming as tar model molecule produced during biomass gasification with an iron/olivine catalyst. *Cr. Chim.* **2010**, *13*, 1319–1325.
30. Jiménez-Morales, I.; Vila, F.; Mariscal, R.; Jiménez-López, A. Hydrogenolysis of glycerol to obtain 1,2-propanediol on Ce-promoted Ni/SBA-15 catalysts. *Appl. Catal. B* **2012**, *117–118*, 253–259.
31. Wang, K.; Li, X.; Ji, S.; Shi, X.; Tang, J. Effect of $Ce_xZr_{1-x}O_2$ promoter on Ni-based SBA-15 catalyst for steam reforming of methane. *Energy Fuel* **2008**, *23*, 25–31.
32. Solsona, B.; Blasco, T.; López Nieto, J.M.; Peña, M.L.; Rey, F.; Vidal-Moya, A. Vanadium oxide supported on mesoporous MCM-41 as selective catalysts in the oxidative dehydrogenation of alkanes. *J. Catal.* **2001**, *203*, 443–452.
33. Vradman, L.; Landau, M.V.; Herskowitz, M.; Ezersky, V.; Talianker, M.; Nikitenko, S.; Koltypin, Y.; Gedanken, A. High loading of short WS₂ slabs inside SBA-15: Promotion with nickel and performance in hydrodesulfurization and hydrogenation. *J. Catal.* **2003**, *213*, 163–175.
34. Hu, X.; Lu, G. Investigation of steam reforming of acetic acid to hydrogen over Ni–Co metal catalyst. *J. Mol. Catal. A* **2007**, *261*, 43–48.
35. Zhang, B.; Tang, X.; Li, Y.; Cai, W.; Xu, Y.; Shen, W. Steam reforming of bio-ethanol for the production of hydrogen over ceria-supported Co, Ir and Ni catalysts. *Catal. Commun.* **2006**, *7*, 367–372.
36. Di Felice, L.; Courson, C.; Foscolo, P.U.; Kiennemann, A. Iron and nickel doped alkaline-earth catalysts for biomass gasification with simultaneous tar reformation and CO₂ capture. *Int. J. Hydrog. Energy* **2011**, *36*, 5296–5310.
37. Bona, S.; Guillén, P.; Alcalde, J.G.; García, L.; Bilbao, R. Toluene steam reforming using coprecipitated Ni/Al catalysts modified with lanthanum or cobalt. *Chem. Eng. J.* **2008**, *137*, 587–597.
38. Xu, X.; Chen, L.; Zhang, X.; Sun, H.; Xu, M. Catalytic conversion of model compounds of biomass tar. *J. Fuel Chem. Technol.* **2009**, doi:10.3969/j.issn.0253-2409.2009.02.023.
39. Świerczyński, D.; Libs, S.; Courson, C.; Kiennemann, A. Steam reforming of tar from a biomass gasification process over Ni/olivine catalyst using toluene as a model compound. *Appl. Catal. B* **2007**, *74*, 211–222.